SEWAGE SLUDGE-DERIVED MATERIALS AS ADSORBENTS OF SO$_2$

Svetlana Bashkova, Andrey Bagreev, David C. Locke[1], and Teresa J. Bandosz

Department of Chemistry, The City College of New York and the Craduate School of City University of New York, New York, N Y 10031,
[1]Department of Chemistry Queens College, CUNY, Flushing, N Y 11367

Introduction

Adsorption of sulfur dioxide on carbonaceous materials has been extensively studied (1-18). Activated carbon and activated carbon fibers have been found to be efficient adsorbents for the low temperature removal of SO$_2$. It is believed that sulfur dioxide is adsorbed with two adsorption energies on activated carbons (3-12). The low energy, about 50 kJ/mol, corresponds to weak physical adsorption, and the second, about 80 kJ/mol, to chemisorption (11). The former process is likely to occur in small pores and is governed by microporosity and the pore size distribution of the activated carbon (12, 13). The strong adsorption is related to the presence of oxygenated groups on the carbon surface (3, 6, 8, 10, 11, 13), which are believed to be catalytic centers for sulfur dioxide oxidation to SO$_3$ (14). Since usually the process is carried out in the presence of moisture and oxygen, sulfur dioxide is oxidized to sulfuric acid as the final product of the reaction. It was also found that three forms of adsorbed sulfur oxides could be present in such a situation. They are as follows: weakly adsorbed SO$_2$, physically adsorbed SO$_3$ (after oxidation of SO$_2$), and strongly adsorbed H$_2$SO$_4$ (5-13).

Recently, we showed that adsorbents obtained from sewage-sludge derived fertilizer can work efficiently as hydrogen sulfide adsorbents (19, 20). Their origin is in biosolids, which are mixtures of exhausted biomass generated in the aerobic and anaerobic digestion of the organic constituents of municipal sewage along with inorganic materials such as sand and metal oxides. Since 6.9 million tons of biosolids (dry basis) were generated in 1998 and only 60% were used beneficially (21), their conversion into useful materials is desirable. The problem of biosolid disposal is of major concern to environmentalists, especially in Europe where the standards for the heavy metal content of sewage sludge-derived fertilizers are 100 times tighter than that in the U.S.A.(21).

The materials obtained from carbonization of dewatered sewage sludge, with or without addition of various activating agents, usually have surface areas between 100 and 500 m^2/g. Reports on their performance as adsorbents of acidic gases differ (22-25). For example, the capacity for the adsorption of SO$_2$ reported by Lu was less than 10% of the capacity of Ajax activated carbon (31). When the performance for H$_2$S adsorption was compared, the capacity of the sludge-derived adsorbents was only 25% of the capacity of Calgon carbon, IVP 4x6 (30). Our recent studies (20) showed that sludge-derived adsorbents have a higher capacity for hydrogen sulfide removal than coconut shell-based carbon, which is considered an alternative to the caustic-impregnated carbons currently used in water treatment plants.

The objective of this study is to determine the sulfur dioxide sorption capacity of sludge-derived adsorbents in comparison with the performance of coconut shell-based activated carbons. Differences in capacities result from differences in porosity, surface chemistry and inorganic constituents of the adsorbents. All of these have an effect not only on the sorption capacity but also on the chemical nature of the oxidation products.

Experimental

Materials

The dewatered sewage sludge-derived product marketed as an organic fertilizer, Terrene®, was obtained from the New York Organic Fertilizer Company (Bronx, New York) in the form of 3 mm diameter granules with an approximately 5% water content. The chemical and structural properties of this sludge product are described elsewhere (19, 20). It contains approximately 35% inorganic matter mainly in the form of iron, aluminum, and silicon oxides and carbonates, and 60% organic matter. The sorbents used in this study were obtained by pyrolysis of Terrene® at temperatures between 400-950°C in a nitrogen atmosphere in a fixed bed (horizontal furnace). The samples are referred to as SC400, SC600, SC800 and SC950 (the numbers represent the pyrolysis temperatures of 400, 600, 800 and 950 °C, respectively.

For comparison, experiments were done using the as-received carbon manufactured from coconut shells by Waterlink Barnebey and Sutcliffe, S208. The sorbent was ground and the granules were the same size as the carbonized Terrene® (1-3 mm).

The prepared materials were studied as adsorbents for sulfur dioxide in the dynamic tests described below under dry and wet conditions. After exhaustion of its adsorbent capacity, each sample is identified by adding the letter "E"

to its designation. Adsorbent samples not subjected to prehumidification (see below) are designated with the letter "D".

Methods

SO₂ breakthrough capacity

Dynamic tests were carried out at room temperature to evaluate the capacity of the sorbents for SO_2 removal under two sets of conditions, wet and dry. For the former, adsorbent samples were packed into a column (length 60 mm, internal diameter 9 mm, bed volume 6 cm³) and prehumidified with moist air (relative humidity 80 % at 25 °C) for one hour. The amount of water adsorbed was estimated from the increase in the sample weight. Moist air (relative humidity 80 % at 25 °C) containing 0.3 % (3,000 ppm) SO_2 was then passed through the column of adsorbent at 0.5 L/min. The breakthrough of SO_2 was monitored using a Micromax monitoring system (Lumidor,) with an electrochemical sensor. The test was stopped at the breakthrough concentration of 350 ppm. The adsorption capacities of each sorbent in terms of mg of SO_2 per g of carbon were calculated by integration of the area above the breakthrough curves, and from the SO_2 concentration in the inlet gas, flow rate, breakthrough time, and mass of sorbent. For each sample the SO_2 test was repeated at least twice. The determined capacities agreed to within 4 %.

To determine the capacity of the dry adsorbent, the experimental conditions were the same as those in the wet run except for the absence of water vapor .

The amount of weakly adsorbed SO_2 was evaluated by purging the adsorbent column with air at 0.5 L/min immediately after the breakthrough experiment. The SO_2 concentration was monitored until its concentration dropped to 5 ppm.

Nitrogen adsorption

Nitrogen adsorption isotherms were measured using an ASAP 2010 analyzer (Micromeritics, Norcross, GA, USA) at -196 °C. Before the experiment the samples were degassed at 120 °C to a constant pressure of 10^{-5} torr. The isotherms were used to calculate the specific surface area, S_{N2}; micropore volume, V_{mic}; total pore volume, V_t; and pore size distribution. All the parameters were determined using Density Functional Theory (DFT) (26, 27). The relative microporosity was calculated as the ratio of the micropore volume to the total pore volume.

pH

A 0.4 g sample of dry adsorbent was added to 20 mL of deionized water and the suspension stirred overnight to reach equilibrium. The sample was filtered and the pH of solution was measured using an Accumet Basic pH meter (Fisher Scientific, Springfield, NJ, USA).

Thermal analysis

Thermal analysis was carried out using TA Instruments Thermal Analyzer (New Castle, DE, USA). The heating rate was 10 °C/min in a nitrogen atmosphere at 100 L/min flow rate.
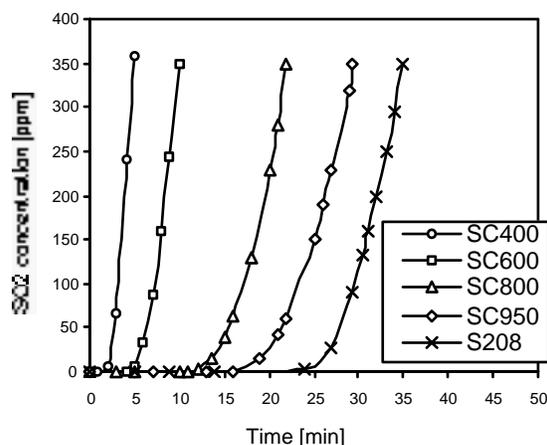
Results and Discussion

Figure 1.

SO₂ breakthrough curves for sludge-derived adsorbents using prehumidification and moist conditions. The breakthrough curve for a coconut shell-derived activated carbon, S208, is included for comparison.

The examples of SO_2 breakthrough curves obtained under wet conditions are presented in Figure 1. For comparison, the curve obtained for the coconut shell-based activated carbon (S208) is included. The values of the adsorbent capacities in mg SO_2 per gram of adsorbent are given in Table 1. The capacity of the wet adsorbent, and to a lesser extent that of the dry material, increased with an increase in carbonization temperature. For the high temperature-carbonized dry sample the SO_2 removal capacity is approximately half that of the wet adsorbent; for these materials, water enhances the adsorption process. In the case of coconut-shell based activated carbon, the presence of moisture has little effect on its SO_2 breakthrough capacity. The results suggest that with increasing carbonization temperature new reactive oxides are formed, e.g. calcium oxide, from decomposition of calcium carbonate (18, 28). Indeed, for the sample obtained at low temperature, SC400, the SO_2 capacities under dry and wet conditions do not differ significantly. However, carbonization at 400 °C would not be expected to completely dehydroxylate the surface inorganic oxides

(29). With increasing carbonization temperature the differences in capacity between the dry and wet conditions increase, suggesting changes in surface chemistry enhanced by the presence of moisture.

Table 1.
Data for the various adsorbents studied under wet and dry (D) conditions: pH before and after exhaustion (E); SO_2 breakthrough capacities, amount of SO_2 desorbed by air purging after breakthrough, and quantity of water adsorbed during prehumidification.

Sample	pH/pH(E)	SO_2 breakthrough capacity (mg/g)	SO_2 desorbed (mg/g)	H_2O adsorbed (mg/g)
SC400	7.0/6.7	5.1	0.41	46.5
SC600	10.6/8.8	9.5	0.23	22.3
SC800	11.3/8.5	22.2	0.20	46.0
SC950	10.7/7.1	29.8	0.20	62.8
SC400D	7.0/7.0	4.8	0.98	---
SC600D	10.6/10.4	12.0	2.33	---
SC800D	11.3/9.5	14.1	2.76	---
SC950D	10.7/8.8	14.5	2.90	---
S208	10.1/2.2	48.2	2.47	72.9
S208/D	10.1/5.8	47.3	10.0	---

The importance of the role of water in the formation of surface species is reflected in the trends in the amount of weakly adsorbed SO_2. For all samples run under dry conditions roughly 20% of the adsorbed SO_2 was removed by air purging. The absence of water precludes the formation of sulfuric acid in the pore system. However, it is possible that SO_2 forms sulfites through reactions with calcium oxide and carbonate. As noted previously (19, 20) the sludge-derived samples contain 3-6 % calcium. For samples run under wet conditions, air purging removes approximately the same amount of SO_2 for all adsorbents except SC400. For all these sludge-derived materials, the site for weak physical adsorption must be the same. About 5% of the SO_2 is weakly adsorbed on the activated carbon, about 5 times more than for the sludge-derived materials. This suggests differences in the mechanism of adsorption on conventional carbons and sludge-derived adsorbents.

These differences in the mechanism are also reflected in the changes in pH of the samples. For the sludge-derived adsorbents a relatively smaller decrease in pH is found after exhaustion, leaving a neutral or slightly basic material. However, a drastic acidification occurs with the activated carbon, presumably caused by the formation of sulfuric acid.
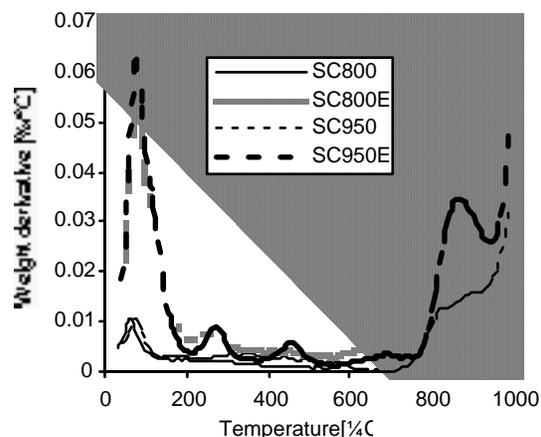

Figure 2.
Differential thermogravimetric (DTG) curves for prehumidified sludge-derived adsorbents before and after exhaustion of sorption capacity with SO_2.

To evaluate the chemical nature of sulfur-containing species, differential thermogravimetric (DTG) experiments were carried out in nitrogen. The examples of DTG curves are presented in Figure 2. Based on reports in the literature on similar systems, the first peak at temperatures less than 150 $^{\circ}$C corresponds to the removal of physically adsorbed water and the weakly adsorbed SO_2 (7, 10, 11, 15-17). The second peak, between 150 and 350 $^{\circ}$C, indicates the presence of strongly adsorbed sulfuric acid (7, 10, 15-17). The third peak, between 350 and 550 $^{\circ}$C, corresponds to dehydroxylation of surface hydroxyl groups (24) and/or volatilization of salts such as $FeSO_4$ (boiling point 480 $^{\circ}$C (30)) that are formed by reaction of metal oxides present in the starting material with adsorbed sulfurous acid. The last peak, between 700 and 900 $^{\circ}$C, results from the decomposition of inorganic salts such as calcium carbonate (decomposition temperatures of aragonite and calcite are 825 $^{\circ}$C and 900 $^{\circ}$C, respectively (30)) and calcium sulfite. Comparison of the DTG curves for the initial samples and the exhausted samples carbonized at T > 600 $^{\circ}$C run under dry conditions shows a significant increase in the size of the first peak. Since no water was present, this increase corresponds to the loss of the weakly adsorbed SO_2. For samples SC800DE and SC950DE, the peak assigned to the strongly adsorbed sulfuric acid is present but its intensity is low because of the absence of water. However, as a result of the reaction of SO_2 under dry conditions with inorganic oxides or salts, the size of the peak near 800-900 $^{\circ}$C increases.

For the exhausted samples run in the presence of moisture, the first peak is much larger than that for the dry-run samples. For the most carbonized material, SC950, which adsorbs the most water and SO_2, the peaks in the exhausted wet-run sample corresponding to loss of sulfuric acid and $FeSO_4$ and/or $CaSO_3$ are well-developed compared to the starting material. These species are not formed at lower temperature of carbonization suggesting unique chemistry of the sludge sample prepared at 950 ^{o}C, producing decomposition of calcium carbonate and possible development of spinel-like structures (2).
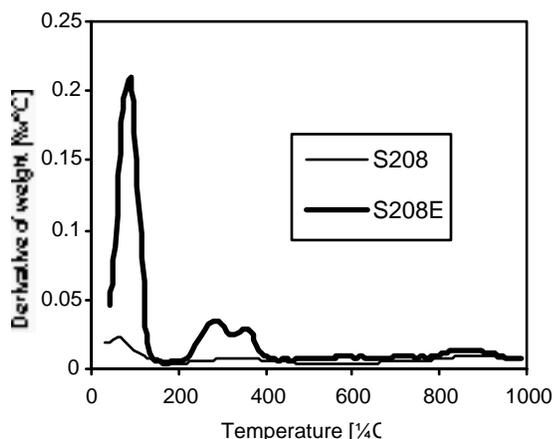

Figure 3.
Differential thermogravimetric (DTG) curves for the prehumidified coconut shell-derived activated carbon.

DTG experiments done on the coconut shell-based carbon revealed a significant weight loss associated with the weakly adsorbed SO_2 and a two-step weight loss between 200 and 400 ^{o}C (Figure 3.). The first of these near 270 ^{o}C results from the removal of surface-adsorbed H_2SO_4 (7, 17). The peak maximizing at 350 ^{o}C probably corresponds to loss of sulfuric acid that is strongly bound to the surface of small pores in the carbon. A similar peak was found in a study of the oxidation of hydrogen sulfide on microporous activated carbons (31, 32). In that study, the bonding with the surface was so strong that extensive water-washing was not able to remove this sulfuric acid.

From the DTG data the weight losses associated with the various forms of sulfur on the carbon surface were calculated. These data are summarized in Table 2, along with the amount of sulfur dioxide adsorbed based on the breakthrough results ($SO_{2(B.Th.)}$) (corrected for the air purge-desorbed amount) and the amount of SO_2 in the form of S(IV) and S (VI) (S_{TA}). The latter was calculated for the dry runs, assuming the first peak in the DTG curves represents loss of SO_2 and the second –loss of H_2SO_4. A

balance had been expected only for the dry runs and the activated carbon, because the first peak area can not be corrected for the contribution of the loss of adsorbed water. In fact it was found that the amount of water desorbed was smaller than the amount adsorbed. This apparent anomaly can be explained by the fact that some of the water adsorbed during prehumidification was consumed by hydration of SO_2 and SO_3 to produce sulfurous and sulfuric acids. These acids can further react with inorganic components of the adsorbents. Water was also consumed in hydroxylation of the surface. For the sludge-derived samples run under wet conditions, the amount of sulfur estimated from the first two DTG peaks is much larger than the amount estimated from the SO_2 breakthrough capacity. The material balance cannot be obtained by considering the contribution of water to the formation of sulfuric or sulfurous acid, salts or surface hydroxides. It should be noted that for the samples run under wet conditions the weight loss between 700 and 900 ^{o}C increased after exhaustion. This indicates that a significant amount of sulfur is present in the form of salts which decompose at temperatures higher than 700 ^{o}C. As expected, the results are different for samples exhausted in dry runs where good balance was found due to the lack of water interference.

Analysis of the nitrogen adsorption isotherms provides information on the spatial deposition of the surface products. The structural parameters calculated from the isotherms are presented in Table 3. During outgassing under high vacuum at 120 ^{o}C, it is likely that the weakly adsorbed SO_2 was removed from the pore system, leaving only sulfuric and sulfurous acid or sulfites and sulfates. The results show a decrease in the surface area and pore volume in the exhausted materials. This decrease is more pronounced for samples carbonized at the higher temperatures. For samples SC800 and SC950 the volume of the micropores was reduced by almost 90%. In Table 3 is also presented the hypothetical volume of sulfur products, V_{sulf}, deposited on the surface assuming their density is 1.83 g/cm^3. For the high temperature-carbonized samples this volume is comparable to the decrease in the volume of the micropores, which indicates the gradual filling of these pores with the products of surface reactions.

A significant decrease in the sorption capacity was also observed for the coconut shell-based activated carbon. As shown by other researchers (5, 13), in the presence of air and moisture, the adsorption of SO_2 by activated carbon with a pH in the basic range is promoted by its conversion to sulfuric acid. That this capacity decrease is greater than the hypothetical volume of acid (assuming that all SO_2 is oxidized to H_2SO_4 of density 1.83 g/cm^3) suggests that the acid is deposited at entrances to the pores.
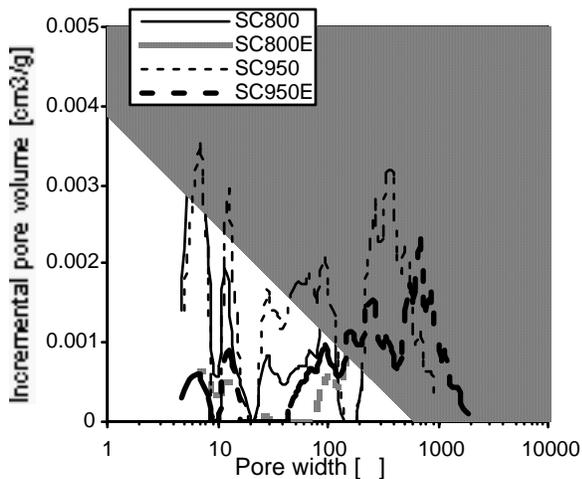
Figure 4.
Pore size distributions for high temperature-carbonized materials before and after exhaustion run under wet conditions.
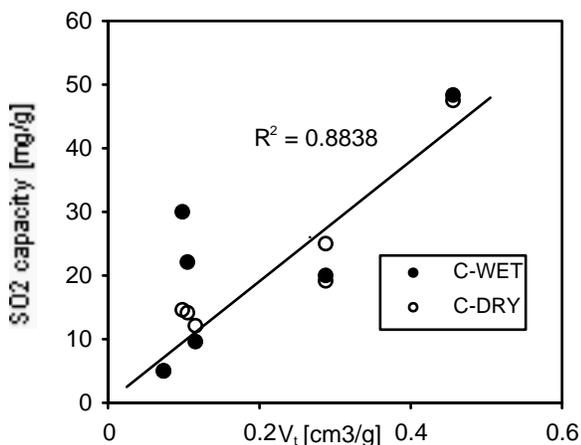

Figure 5.
Dependence of the SO_2 capacity on the total pore volume of the adsorbents. The line and the correlation coefficient refer to the data obtained under dry conditions (open circles).

These changes are seen in the pore size distributions presented in Figure 4. The very narrow first peaks centered at about 6 Å with high intensities indicates the presence of fine microporosity, probably within the carbonaceous deposit of the initial materials (19). After the adsorption process the volume in these pores is significantly decreased from the blocking of the pore entrances as is shown in Table 2. Pores similar in size to the SO_2

molecule should be especially active in the process of physical adsorption of sulfur dioxide. Indeed, the plot presented in Figure 5 clearly shows that for the dry run samples, where a chemical reaction with surface oxides is less probable, a good correlation is found ($R^2 = 0.88$ for the dry run points) between the amount of SO_2 adsorbed and total pore volume (points corresponding to SO_2 adsorption on peat based Norit[®] carbon, R2030, with V_t=0.282 cm^3/g are added to better demonstrate the trend observed). For the wet run the correlation is not as good, probably because of the catalytic effect of the surface of the adsorbents.

The catalytic effect of the surface chemistry of the sludge-derived materials on the normalized capacity (capacity per unit surface area of adsorbent) is visualized in Figure 6. The normalized capacity of the sludge-derived adsorbents, especially those produced at higher temperature, is much larger than that of the activated carbon. The significantly higher activity of the surfaces of the adsorbents carbonized at 800 ^{o}C and 950 ^{o}C probably result from the combined effect of dehydroxylation of inorganic phase oxides and their solid state reactions promoted at high temperature and reducing conditions. It is possible that a spinel-like structure is formed with a high dispersion of metals.
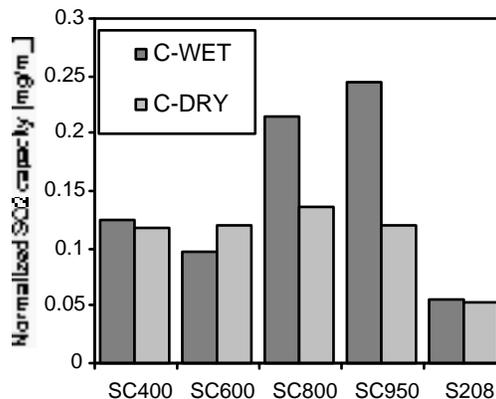

Figure 6.
Normalized capacity of the samples for SO_2 under wet and dry conditions.

Conclusions

The results presented in this paper demonstrate that sewage-sludge derived materials can work efficiently as adsorbents for sulfur dioxide from moist air. The SO_2 on the surface of these materials is first physically adsorbed, oxidized to SO_3 and then converted into sulfuric acid. The acid reacts with inorganic oxides and/or salts to create soluble sulfates. The samples carbonized at higher

temperatures are more active because of the presence of chemically active calcium oxides and spinel-like structures with high dispersion of metals.

References

1. Kohl A, Riesenfeld F. Gas Purification. 4th edn., Gulf Publishing Company, Houston, 1985.
2. Stirling D. The Sulfur Problem: Cleaning up Industrial Feedstocks. The Royal Society of Chemistry, Cambridge, UK, 2000.
3. Rodriguez-Mirasol J, Cordero T, Rodriguez JJ. Abstract of 23rd Biennial Conference on Carbon, 18-23 July 1997, College Park, PA, p. 376.
4. Moreno-Castilla C, Carrasco-Marin F, Utrera-Hidalgo E, Rivera-Utrilla J. Langmuir 1993; 9: 1378.
5. Lisovskii A, Shter GE, Semiat R, Aharoni C. Carbon 1997; 35: 1645.
6. Davini P. Carbon 1991; 29: 321.
7. Mochida I, Miyamoto S, Kuroda K, Kawano S, Yatsunami S, Korai Y, Yatsutake A, Yashikawa M. Energy & Fuels 1999; 13: 369.
8. Davini P. Carbon 1990; 28: 565.
9. Lisovskii A, Semiat R, Aharoni C. Carbon 1997; 35: 1639.
10. Anurov CA, Keltsev NV, Smola VI (Uspekhi Khimii) Russian Chemical Reviews 1977; 46: 33.
11. Raymundo-Piñero E, Cazola-Amorós D, Salinas-Martinez de Lecea C Linares-Solano A. Carbon 2000; 38: 335.
12. Molina-Sabio M, Muñecas,….?? Rodriguez-Reinoso, F, McEnaney B. Carbon 1995; 33: 1777.
13. Daley MA, Mangun CL, DeBarr JA, Riha S, Lizzio AA, Donnals GL, Economy J. Carbon 1997; 35: 411.
14. Lizzio AA, DeBarr JA. Energy and Fuels 1997; 11: 284.
15. Rubio B, Izquierdo MT. Carbon 1997; 35: 1005.
16. Rubio B, Izquierdo MT, Mastral AM. Carbon 1998; 36: 263.
17. Mochida I, Miyamoto S, Kuroda K, Kawano S, Yatsunami S, Korai Y, Yatsutake A, Yashikawa M. Energy & Fuels 1999; 13: 374.
18. Przepiórski J, Yoshida S, Oya A. Carbon 1999; 37: 1881.
19. Bagreev A, Locke DC, Bandosz TJ. Carbon, in press.
20. Bagreev A, Bashkova S, Locke DC, Bandosz TJ. Environ. Sci. Technol, submitted.
21. Biosolid Generation, Use, and Disposal in The United States: EPA530-R-99-009, September 1999.
22. Chiang PC, You JH. Can. J. Chem. Eng. 1987; 65: 922.
23. Lu GQ, Low JCF, Liu CY, Lau AC. Fuel 1995; 74: 3444.
24. Lu GQ, Lau DD. Gas Sep. Purif. 1996; 10: 103.
25. Lu GQ. Environ. Tech. 1995; 16: 495.
26. Lastoskie CM, Gubbins KE, Quirke N. J. Phys. Chem. 1993; 97: 4786.
27. Olivier JP. J. Porous Materials 1995; *2*: 9.
28. Ho C-S, Shih S-M. Ind. Eng. Chem. Res. 1992; 31: 1130.
29. Barrer RM. Zeolites and Clay Minerals as Sorbents and Molecular Sieves; Academic Press: London, 1978.
30. Handbook of Chemistry and Physics, 67th ed.,Weast, R.C. Ed. CRC press, Boca Raton, Fl, 1986.
31. Adib F, Bagreev A, Bandosz TJ. Ind. Eng. Chem. Res. 2000; 39: 2439.
32. Bagreeev A, Rahman H, Bandosz TJ. Advances in Environmental Research, in press.

Table 2.
Weight loss (%) at the indicated temperature ranges related to the presence of the products of SO_2 deposition/reaction on the surface and estimated amount of sulfur dioxide from the breakthrough capacity test $(SO_{2(B.TH.)})$ (%) and thermogravimetric experiments $SO_{2(TA)}$. (%).

Sample	<150 ^{o}C (SO$_2$)	150-350 ^{o}C (H$_2$SO$_4$)	350-550 ^{o}C (H$_2$O)	550-700 ^{o}C	700-900 ^{o}C	SO$_{2(TA)}$	SO$_{2(B.Th))}$.
SC400	1.44	3.11	6.51	4.98	8.11	---	---
SC400E	3.73	3.67	7.21	5.17	7.63	---	0.47
SC400DE	1.69	1.94	6.76	5.27	8.25	0.25	0.38
SC600	1.73	1.34	1.83	298	8.88	---	0.93
SC600E	3.48	1.96	1.91	3.70	8.94	---	0.93
SC600DE	1.85	1.69	1.95	2.91	9.12	0.35	0.96
SC800	0.67	0.63	0.23	0.14	4.59	---	---
SC800E	3.46	1.40	0.74	0.58	5.06	---	2.20
SC800DE	1.69	1.06	0.58	0.24	5.50	1.30	1.13
SC950	0.67	0.12	0.01	0.00	1.62	---	---
SC950E	4.20	1.17	0.64	0.33	3.29	---	2.97
SC950DE	2.00	0.52	0.09	0.00	2.06	1.39	1.16
S208	1.78	1.15	0.79	0.62	1.46	---	---
S208E	11.59	4.8	2.14	1.29	2.18	---	4.57
S208DE	1.45	2.26*	0.39	1.50	1.98	1.95	2.98

* peak between 150-400 ^{o}C

Table 3.
Structural parameters calculated from nitrogen adsorption isotherms, and estimated hypothetical volume of sulfur species (assuming density equal to 1.83 g/cm^3).

Sample	S_{BET} (m^2/g)	S_{DFT} (m^2/g)	V_{mic}(DFT) (cm^3/g)	V_t (cm^3/g)	V_{mic}/V_t	ΔV_{mic} (cm^3/g)	V_{sulf} (cm^3/g)
SC400	41	21	0.006	0.075	0.080		
SC400E	11	7	0.003	0.055	0.055	0.003	0.004
SC600	99	92	0.030	0.115	0.261		
SC600E	11	8	0.003	0.049	0.061	0.027	0.008
SC800	104	106	0.033	0.107	0.308		
SC800E	30	27	0.008	0.056	0.143	0.025	0.019
SC950	122	104	0.028	0.100	0.280		
SC950E	39	32	0.007	0.053	0.132	0.021	0.025
S208	880	889	0.359	0.457	0.786		
S208E	690	690	0.280	0.296	0.946	0.079	0.040